Author Manuscript

Author Manuscript

Author Manuscript

Author Manuscript

HHS Public Access

Author manuscript

Environ Sci Technol. Author manuscript; available in PMC 2017 August 23.

Published in final edited form as:

Environ Sci Technol. 2016 November 01; 50(21): 11539–11548. doi:10.1021/acs.est.6b03092.

Post Gold King Mine spill investigation of metal stability in water and sediments of the Animas River watershed

Lucia Rodriguez-Freire[1], **Sumant Avasarala**[1], **Abdul-Mehdi S. Ali**[2], **Diane Agnew**[3], **Joseph H. Hoover**[4], **Kateryna Artyushkova**[5], **Drew E. Latta**[6], **Eric J. Peterson**[5], **Johnnye Lewis**[4], **Laura J. Crossey**[2], **Adrian J. Brearley**[2], and **José M. Cerrato**[1,*]

[1]Department of Civil Engineering, MSC01 1070, University of New Mexico, Albuquerque, New Mexico 87131, United States

[2]Department of Earth and Planetary Sciences, MSC03 2040, University of New Mexico, Albuquerque, New Mexico 87131, United States

[3]New Mexico Environment Department, 121 Tijeras Avenue NE, Albuquerque, New Mexico 87102, United States

[4]Community Environmental Health Program, MSC09 5360, University of New Mexico, Albuquerque, NM 87131, United States

[5]Department of Chemical and Biological Engineering, MSC01 1120, University of New Mexico, Albuquerque, New Mexico 87131, United States

[6]Department of Civil and Environmental Engineering, The University of Iowa, 4105 Seamans Center, Iowa City, Iowa 52242, United States

Abstract

We applied spectroscopy, microscopy, diffraction, and aqueous chemistry methods to investigate the persistence of metals in water and sediments from the Animas River 13 days after the Gold King Mine spill (August 5, 2015). The Upper Animas River watershed, located in San Juan CO, is heavily mineralized and impacted by acid mine drainage, with low pH water and elevated metal concentrations in sediments (108.4±1.8 mg kg^{-1} Pb, 32.4±0.5 mg kg^{-1} Cu, 729.6±5.7 mg kg^{-1} Zn and 51,314.6±295.4 mg kg^{-1} Fe). Phosphate and nitrogen species were detected in water and sediment samples from Farmington, NM, an intensive agricultural area downstream from the Animas River, while metal concentrations were low compared to those observed upstream. Solid-phase analyses of sediments suggest that Pb, Cu, and Zn are associated with metal-bearing jarosite and other minerals (*e.g.* clays, Fe-(oxy)hydroxides). The solubility of jarosite at near-neutral pH and biogeochemical processes occurring downstream could affect the stability of metal-bearing minerals in river sediments. This study contributes relevant information about the association of metal mixtures in a heavy mineralized semi-arid region, providing a foundation to better understand long-term metal release in a public and agricultural water supply.

*Corresponding jcerrato@unm.edu, Telephone: (001) (505) 277-0870, Fax: (001) (505) 277-1988.

Supporting Information Available

Additional materials and methods, eight additional tables (S1 to S8), and seven additional figures (S1 to S7) are presented. This material is available free of charge via the Internet at http://pubs.acs.org.

Author Manuscript
Author Manuscript
Author Manuscript
Author Manuscript

TOC Art

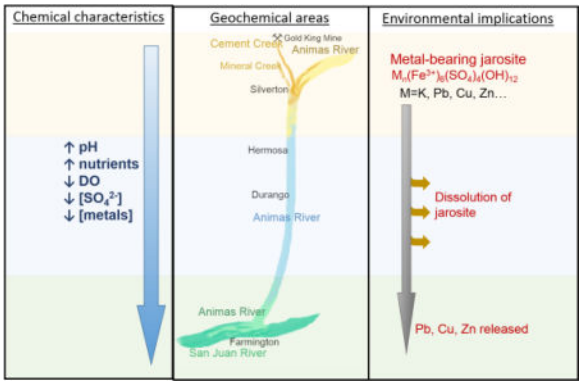

Introduction

Effects of mining legacy are a worldwide concern due to contamination of water, soil, and diverse ecosystems. Acid mine drainage (AMD) is continuously produced and discharged into the environment from abandoned mines (AM). The worldwide cost of treating AMD is estimated in the tens of billions of dollars.[1] The AM land inventory in the United States has listed over 28,000 AM sites and over 70,000 features as of 2011, 75% of these sites still need to be investigated and/or remediated.[2] More than 1,500 AM are located in the San Juan Mountains affecting the Animas River (AR) watershed in Colorado.[3]

The Upper AR watershed is an extensively mineralized area comprising the northern-most headwaters of the AR in San Juan County, CO, and its two main tributaries, Cement Creek (CC) and Mineral Creek (MC) (Figure 1). Natural mineralization is a fundamental source of metals (copper, Cu; arsenic, As; lead, Pb; zinc, Zn; gold, Au)[4–7] and sulfides in the Upper AR,[8] with background stream water pH values between 2.6–8.5, sulfate (SO_4^{2-}) concentrations ranging from 1–1,300 mg l^{-1}, and Zn concentrations between <20–14,300 μg l^{-1}.[9] Mining exploitation of the Upper AR watershed started in 1871.[7] During the 120 years of active mining, 48% of the total mill tailings production was released into streams throughout the watershed (8.6 million short-tons). The AMD has pH values between 2.35–7.77, SO_4^{2-} ranging between 45–2,720 mg l^{-1} and Zn concentrations of <20–228,000 μg l^{-1}.[9] Two major spill accidents occurred in 1974 and 1978 prior to the GKM spill in 2015, releasing hundreds of thousands of gallons of AMD into the AR.[10] On August 5, 2015, at the Gold King Mine (GKM) in San Juan County, CO, a wall of unconsolidated mine waste was breached causing the release of 3 million gallons of AMD into CC[10], an AR tributary, which served as the motivation for this study.

The AMD contamination in the AR has global impacts as the AR flows southbound from the San Juan Mountains, CO, to Farmington, NM, where it discharges into the San Juan River (SJR); the SJR moves westbound to the Colorado River at the Lake Powell, UT. Moreover, the SJR is the main water source for the largest Navajo farming operation (Navajo Agricultural Products Industry, NAPI). As the AR travels through different environmentally relevant conditions (from heavily mineralized to intensive agricultural areas), the transported

Author Manuscript Author Manuscript Author Manuscript Author Manuscript

sediments will be affected by various biogeochemical processes that can cause metal mobilization. The oxidative weathering of pyrite and other Fe(II)-sulfides results in: a) AMD production;[11] b) formation of secondary minerals such as jarosite, goethite, and other Fe(III)-minerals which can sequester trace metals.[12–14] The dissolution of these metal-bearing minerals can cause the release of sequestered metals (*e.g.* As, Pb, and others) due to biotic and abiotic interactions.[15–17] The specific mechanisms governing the transformation of complex metal mixtures in the environment remain unclear and it is a major research challenge.[13, 18, 19]

The objective of this study is to investigate the stability of metal mixtures on samples collected on August 17–18, 2015, after the GKM spill. The Animas River is a complex system affected by natural mineralization, mining events and extensive agriculture. We integrated spectroscopy, microscopy, diffraction, and water chemistry techniques to identify specific mineralogical and water quality features affecting metal (im)mobilization in the Animas River watershed, a primary drinking and agricultural water source for Colorado, New Mexico, and Utah. The results of this investigation set the foundation to further understand the complex mechanisms influencing the fate of metals in a surface water basin affected by varying environmental conditions in a semi-arid region.

Materials and Methods

Sampling locations

We collected water and sediment samples in locations throughout the AR watershed (Figure 1) on August 17–18, 2015, where possible selecting locations proximal to EPA sampling locations. Our sampling sites include a location in CC (sample ID L1, in a similar location named CC48 by EPA). Another location was selected on the AR, upstream of its confluence with CC, (Sample ID L2, A68 by EPA) with the intent of obtaining a reference sample that was not affected by the GKM spill. The remaining locations were in the AR downstream of CC, which include Silverton, CO (Sample ID L3, A72 by EPA), Baker's Bridge, CO (BB, Sample ID L4, Baker's Bridge by EPA), Cedar Hill, NM (Sample ID L5, ADW-022 by EPA), Farmington, NM (Sample ID L6, FW40 by EPA); and a sample in the SJR near Farmington, NM (Sample ID L7). Two sediment samples were obtained a few feet above the water river level in CC (Sample ID C1) and in the AR near Farmington, NM (Sample ID C6).

Sampling procedure

Field measurements of the pH, ORP, dissolved oxygen (DO), and specific conductivity (SC) were performed using a field meter (YSI Pro Plus multi-parameter). Unfiltered water samples were collected in 500 ml Nalgene bottles from the middle of the stream. 60 ml syringes and 0.45 μm filters (25 mm PTFE Membrane syringe filter) were used to filter water samples into 125 ml Nalgene bottles. Additionally, filtered water samples were acidified by adding 6–8 drops of ultra-high purity concentrated nitric acid (HNO_3). Sediment samples were collected from the submerged banks of the stream and away from the water level (C1 and C6) using a trowel and then dumping the sample into plastic bags. Water and sediment with water samples were preserved on ice in a cooler.

Author Manuscript Author Manuscript Author Manuscript Author Manuscript

Analytical methods

Water and sediment samples were analyzed using a variety of techniques. A detail description of the methods is presented in the Supplementary Information, SI. Briefly, ion chromatography was used to measure anion concentration in the water samples. Inductively-coupled plasma (ICP), optical emission spectrometry (OES) or mass spectrometry (MS) were used to measure the total element concentrations in the samples. Solid samples were further analyzed using X-ray fluorescence (XRF), X-ray photoelectron spectroscopy (XPS), X-ray diffraction (XRD), scanning transmission electron microscopy (STEM), and Mössbauer spectroscopy.

Results and Discussion

Chemical analyses for surface water

Analyses of EPA water quality data[20] collected following the GKM spill indicates elevated metal concentrations in CC and the AR immediately after the spill; and periodic increases in total metal concentrations more than 2 months after the spill (Figure S1). Peak concentrations of As and Pb exceeded national drinking water standards (10 μg l^{-1} and 15 μg l^{-1}, respectively) following high flow-events downstream the AR.[21] Along the Colorado stretch of the AR, the periodic increases in total metal concentrations are muted, likely due to the influence of topography on the river's ability to carry suspended sediment. More prominent increases in metal concentrations were observed along the New Mexico stretch of the AR before its confluence with the SJR in Farmington, NM. Metal concentrations for the water samples we collected on August 17–18, 2015 were all low (below the national drinking water standards). No major precipitation events occurred after the spill and before sample collection, so the result obtained is consistent with the analyses of EPA water quality data presented above.

The difference between the background parent-rock material and the land use will also affect the total, dissolved and suspended metal concentrations (Figure S2 and Table S1 in the SI), and other water quality parameters such as pH, DO, dissolved anions and cations (Figure S3), and SC (Table S2 in the SI). The highest total concentration for some metals was found in the CC sample, L1 (*i.e.* 13.41 mg l^{-1} Fe, 54.92 μg l^{-1} Cu and 2.94 mg l^{-1} Zn) mostly as dissolved metals, corresponding with the lowest pH (3.32), the greatest DO (10.3 mg l^{-1}) and SO_4^{2-} (630.5 mg l^{-1}) concentrations, and the highest SC (1,000 μS cm^{-1}). Total metal and DO concentrations decreased and the fraction of suspended metals and pH increased downstream, reaching values of 0.54 mg l^{-1} Fe, 1.61 μg l^{-1} Cu, non-detected Zn, 3.3 mg l^{-1} DO, and pH 7.95–8.14 in the Farmington area. SO_4^{2-} concentration was the lowest in the AR upstream the confluence with CC (86.6 mg l^{-1} in L2), increasing just after the confluence (170.9 mg l^{-1} in L3) and decreasing further downstream. In contrast, Pb concentration was the highest in the AR after the confluence with CC where most of the Pb was 99% suspended (3.33 μg l^{-1} Pb in CC, L1, vs. 4.14 μg l^{-1} Pb in the AR after the confluence, L3). Some major cations (e.g. Mg, K, Na, Ba) and metals (e.g. Sr, Mo, V) did not follow the same concentration profile (Table S1). For example, uranium (U) concentration was the highest in the AR near Farmington sample (0.25 μg l^{-1} U in L6 compared with 0.11 μg l-1 U in CC, L1). Finally, detectable concentrations of phosphate

Author Manuscript Author Manuscript Author Manuscript Author Manuscript

(2.6 mg l^{-1} PO_4^{3-}), nitrate (24.4 mg l^{-1} NO_3^-) and nitrite (0.9 mg l^{-1} NO_2^-) were only detected downstream of the AR confluence in the SJR, Farmington area, L7.

Our measurements are consistent with previous studies indicating that the water quality is different in CC compared with the Farmington area. In September 30, 1998, the pH was measured to be 3.78 in CC and 7.27 and 6.73 in the AR before and after the confluence with CC.[22] Similarly, in the same study, the SC was 963 μS cm^{-1} in CC, and 295 μS cm^{-1} and 440 μS cm^{-1} in the AR.[22] The difference in water quality between CC and the AR upstream of the confluence has been observed in a previous study, and it is probably explained by a larger propylitic area in the AR basin, with higher calcite and lower sulfide concentrations than in CC.[23] The pH values in the AR and SJR near Farmington varied from a minimum of 6.9 to a maximum of 9.5 since the monitoring by the U.S. Geological Survey (USGS) began in 1955,[24, 25] with an average pH of 7.89 ±0.37 in the AR and 7.85 ±0.32 in the SJR. Additionally, the measurements of SC near Farmington show a great variation, ranging from 101 to 2290 μS cm^{-1}.[24, 25]

The fact that elevated concentrations of metals of environmental relevance are predominantly present as suspended solids in the water highlights the importance of studying the sediment composition and mineralogy in the AR. We have used an array of techniques to further investigate the chemical composition, structure, and morphology of these sediments.

Chemical analyses for sediments

Elevated metal concentrations were detected by chemical analyses in sediments along different locations of the AR. Natural mineralization and high mining activity have caused a widespread distribution of metals in the area. Bulk concentration analyses (Table S3 in SI) performed with X-Ray Fluorescence (XRF) showed that Pb, S, Cu and P concentration decreases from CC, L1, (2620 mg kg^{-1} Pb, 13750 mg kg^{-1} S, 686 mg kg^{-1} Cu, 3125 mg kg^{-1} P) to the AR near Farmington sample (72 mg kg^{-1} Pb, 491 mg kg^{-1} S, less 30 mg kg^{-1} Cu, 600 mg kg^{-1} P). Interestingly, the concentrations of Fe, Mn and Zn were higher in the sample, C1, collected above the water level in the same area, than in L1. Furthermore, Fe, Mn and Zn concentrations are the highest in the AR sediments after the confluence with CC (L3) than in the CC sample (L1), which suggests a different source of these elements in those locations, most likely from different mineral assemblages in MC or upstream the AR.[26] Overall, the metal concentrations in the sediments from the Silverton area are above their average concentrations in the earth's crust of 55 mg kg^{-1} Cu, 56.3 g kg^{-1} Fe, 950 mg kg^{-1} Mn, 12.5 mg kg^{-1} Pb, 260 mg kg^{-1} S and 70 mg kg^{-1} Zn.[27] Our results are in agreement with previous studies reporting that the concentration of metals in the sediments in the Upper AR watershed exceeded the average crustal earth concentration.[28] Therefore, the concentrations found in the sediments in the AR after the GKM spill are within ranges shown by the historical data available for the site.

The trends in elemental composition observed with XRF are consistent with results obtained from acid digestions to determine the acid extractable elemental content in sediments. Figure 2 shows the concentration profile of selected elements along the sampling locations, and Table S4 in SI presents the average concentrations and standard deviations for all the

Author Manuscript Author Manuscript Author Manuscript Author Manuscript

measured elements. Arsenic, cadmium (Cd), mercury (Hg) and other trace elements now were detected in the sediments due to the lower detection limit of the method. Arsenic concentration decreased from 4.25 ±0.25 mg kg^{-1} As in CC to 0.22 ±0.00 mg kg^{-1} As in the SJR. Although, the measured As concentration can be considered low for the area where they have been measured to range from 15 to 30 mg kg^{-1},[28] our results are from a partial acid digestion. The Cd concentration profile is similar to those described for Fe, Mn and Zn; the highest concentration was measured in the AR just below the confluence with CC (0.66 ± 0.01 mg kg^{-1} Cd) and the concentration then decreases downstream to values of 0.04 ±0.00 mg kg^{-1} Cd in the Farmington area. Finally, Hg concentration in CC of 86.7 μg kg^{-1} was slightly above the average crustal earth concentration of 80 μg kg^{-1},[27] decreasing downstream along the AR. In addition, trace concentrations of U and V (Table S4 in SI) were measured in the sediments in all sampling locations, with the highest U and V concentrations, 0.28 ±0.04 mg kg^{-1} U and 4.7 ±0.2 mg kg^{-1} V, detected in the AR at BB, CO. The slight increase in U and V concentration near BB could be explained by higher natural U concentration in the area[29] and the former presence of an ore processing facility located a quarter of a mile southwest of the city of BB which produced V from 1942 to 1946 and U from 1949 to 1963, producing 917,466 m^3 of mill tailings.[30]

Surface analyses for metal oxidation states and nutrient speciation in sediments

Additional solid analyses were performed in solid samples L1, L4, and L7, which are selected as a representation of the AR watershed from Silverton, CO, to Farmington, NM. We investigated the metal speciation in the near surface region of the sediments (top 5 – 10 nm depth) using XPS. Lead(II), Fe(II), and SO_4^{2-} were predominant in samples collected from CC (sample L1) and BB (sample L4). In contrast, Fe(III) and the presence of phosphate, NO_3, NO_2, NH_3, and SO_4^{2-} were predominant in the sediment samples from Farmington (sample L7). The oxidation state and chemical composition data measured by XPS analyses are consistent with the observed differences for chemical analyses of water and sediments in the areas of CC, BB, and Farmington, discussed in the previous subsections.

The near-surface region of the sediments from CC have the highest concentration of metals and predominance of reduced Fe. As shown in Figure 3, the Pb 4f doublet peaks ($4f_{7/2}$ and $4f_{5/2}$) are clearly detected in samples L1 and L4. No Pb was detected in C1 or in sample L7. The better S/N of the Pb 4f spectrum in sample L1 compared with L4 indicates a higher surface Pb concentration upstream, in agreement with the bulk analyses by XRF and acid digestion. Lead is present as 100% Pb(II) in sample L1, but in sample L4 Pb is 82.2% Pb(II). Iron was detected in all the sediment samples by Fe 3p XPS narrow scans (Figure 3). Curve fitting of Fe 3p spectra suggest that the surface region of the sediments from CC and BB consist of 72.1 ±7.0% Fe(II) (C1: 64.0% Fe(II); L1: 75.9% Fe(II), L4: 76.3% Fe(II)). In contrast, Fe is mostly oxidized in the surface of the sediments from Farmington (L7, 12.0% Fe(II) and 88.0% Fe(III)). A summary of the XPS curve-fit results is presented in Table S5 in SI. Interestingly, Mn and Zn were measured in high concentrations in bulk analyses of sediments, but were not detected in the near-surface region of the sediments samples with XPS.

Author Manuscript Author Manuscript Author Manuscript Author Manuscript

Sulfur, P and N species present in the surface of the sediments were also identified with XPS, following a trend similar to their concentration profile in the water samples. Sulfur (Figure S4) was found as SO_4^{2-} in the samples from upstream the AR in CC (L1) and BB (L4), but not in C1 or in the Farmington sample (L7). High SO_4^{2-} concentration was also measured in the water sample from CC; these results together are in agreement with the geology of the area and the high sulfidic minerals found in the Red Mountains[5] and SO_4^{2-} minerals in the caldera.[31] Phosphorous was present as PO_4^{3-} (100%) in all the analyzed sediments, but it was only detected in the water sample from Farmington. Finally, N species in the sediments were characterized and their spectra are shown in Figure S5. Reduced amide ($-NH_2$) and ammonia ($-NH_3$) groups were detected in the four sediment samples, from CC to Farmington. In the sample from Farmington, $-NO_3$ (34.3%) and $-NO_2$ (9.8%) groups were found in the sediments together with the highest percentage of reduced N-species (L4, 95% $-NH_2$ and 5% $-NH_3$); similarly, the anions NO_3^- and NO_2^- were only detected in the water sample from Farmington, where they occurred with PO_4^{3-}.

Sediment mineralogy

Microscopy, spectroscopy, and XRD analyses of sediments collected from CC (L1) and Baker's Bridge (L4) suggest that metals such as Pb, Cu, and Zn are associated with Fe-SO_4^{2-} as well as Fe-oxide and -oxyhydroxide phases. The mineral composition of these sediments was analyzed using a combination of STEM-EDX and XRD. STEM X-ray maps and EDS spectra obtained for sediment sample L1 are illustrated in Figure 4A. The sediment sample contains abundant submicron, euhedral to anhedral crystals containing Fe, Cu, S, O, P and K consistent with the presence of Cu-bearing jarosite. The Cu-bearing jarosite grains are compositionally variable, with some grains containing detectable concentrations of Zn and Pb, whereas in other grains these elements are not detectable by EDS (Figure 4A). Crystals of Cu-Pb-Zn-bearing jarosite were also detected in sample L4 (Figure S6). The jarosite grains commonly present are associated with muscovite or illite, the predominant minerals in these sediments. Lead, Zn and P are commonly also associated with Fe-oxides or -oxyhydroxides and are likely absorbed and/or co-precipitated onto the surfaces of the Fe-oxide grains. The STEM results are consistent with XRD analyses. XRD patterns for the sediment samples L1 and L4 are illustrated in Figure 4B and a summary of the quantitative analyses for these patterns is presented in Table S6. The major minerals in the samples are quartz (SiO_2, 37.1% L1 and 36.8% L4), illite [$(Al,Mg,Fe)_2(Si,Al)_4O_{10}(OH)_2$,($H_2O$), 29.9% L1 and 12.1% L4] and chlorite [$(Mg,Fe)_3(Si,Al)_4O_{10}(OH)_2 \cdot (Mg,Fe)_3(OH)_6$, 17.6% L1 and 10.7% L4]. Hydronium-jarosite was only confirmed in the sample from CC (7.4% L1). Other studies have also found an association of metals with jarosite phases ($M_n(Fe^{3+})_6(SO_4)_4(OH)_{12}$ mineral phases, where M may be K, $(NH_4)^+$, Na, Ag or Pb and n = 1 for divalent cations, and n=2 for monovalent cations), with the occurrence of Pb mostly in anhedral jarosite.[32, 33]

Mössbauer spectroscopy analyses were used to further identify Fe-bearing minerals in sediments from CC (C1 and L1) and from BB (L4). The Mössbauer spectra are shown in Figure 3 and a summary of parameters and results is presented in Table S7 (a more detailed explanation of is included in the SI). The Mössbauer parameters for sample C1 (Figure 5A) are consistent with those of nano-crystalline goethite.[34–36] Additional Fe-bearing minerals

Author Manuscript Author Manuscript Author Manuscript Author Manuscript

detected in C1 are weakly-ferromagnetic hematite, a paramagnetic Fe(III) doublet feature which is consistent with any number of Fe(III) containing minerals, including primary silicates and clay minerals,[35, 37] and a paramagnetic octahedral Fe(II) doublet feature consistent with Fe(II) in clay minerals, primary silicates, phosphates, or sulfates.[37] The Mössbauer parameters for the Fe(II) are consistent with the XRD identification of chlorite and illite type clay minerals. Samples L1 (Figure 5B) and L4 (Figure 5C) have similar paramagnetic Fe(III) doublets consistent with octahedral Fe(III) in silicates, and phosphates[37, 38] and nano-crystalline goethite. In addition to goethite, sample L4 contains weakly-ferromagnetic hematite, consistent with the detection of hematite in the control sample.[34, 35] Also, an additional Fe-bearing phase was detected in samples L1 and L4, which based on XRD and STEM data, is most likely jarosite. There is limited information about the low temperature Mössbauer parameters of jarosite-group Fe-minerals. In order to resolve this discrepancy, we synthesized K-jarosite following the procedure described elsewhere,[39] confirmed its identity with XRD, and collected Mössbauer spectra (Figure S7A). The synthetic jarosite hyperfine parameters and temperature behavior are consistent with a portion of the Fe in samples L1 and L4. By fitting room temperature spectra (Figure S7B), we estimate that 20–35% of the Fe present in the two samples is present as jarosite.

Relevant geochemical features

The difference between the background parent-rock material and land use affected the metal concentration profiles and other water quality parameters such as pH, DO, and dissolved anions and cations, resulting in three distinct areas along the AR watershed. *The first area* comprises the Upper AR watershed which is heavily mineralized and impacted by AMD. The water in the area is characterized by low pH, high SC and high DO and SO_4^{2-} concentration. Water and sediments in this first area contain high concentrations of Fe, Mn, Cu, Pb and Zn, consistent with other literature.[7, 28, 40] *The second area* is the Animas River, between Silverton, CO, and Farmington, NM. The water is characterized by increasing pH and alkalinity, and decreasing, SC, DO. Sediments and water have lower concentrations of Fe, Mn, Cu, Pb and Zn, but higher U and V concentrations due to the legacy contamination.[30] *The third area* is near Farmington, NM, where metal concentrations in the water and sediments are low, and nutrients are present due to intense agricultural activities in this zone. In contrast with the Silverton reach, the samples from Farmington have low total metal, SO_4^{2-} and DO and high pH (7.95 – 8.14) and alkalinity. In addition, phosphates and N-species were only found in water and sediments of the Farmington area.

The three different geochemical areas are the result of various source contributions, such as natural mineralization, mining and/or agricultural activity. Cement Creek is a heavily mineralized area,[7, 8] while Farmington is an agriculture-intensive zone with more than 500 farms with nearly 70,000 irrigated acres of farmland.[41] The use of fertilizers and manure is known to increase the N and P loads in water affected by agricultural run-off,[42] as it is observed in the SJR with the presence of NO_3^-, NO_2^- and PO_4^{3-} near Farmington. The decrease in total metal concentration downstream the AR could be explained by simple dilution[26] but also by the deposition of the suspended metals or their immobilization within the river sediments by physical or chemical mechanisms (sorption and/or precipitation). The deposited or immobilized sediments can become mobilized as evidenced by the increase in

Author Manuscript Author Manuscript Author Manuscript Author Manuscript

As and Pb total concentrations in water following high-flow events. These spikes in metal concentration in water occurring in the Farmington area are of special concern since the water is used for irrigation of agriculture lands, and the potential for metal-accumulation in edible plants.[43–45]

Finally, the identification of Fe-bearing minerals, such as jarosite phases, in this study's sediments has important implications to the fate of metals in the AR. The identification of jarosite in the Upper AR basin[46] was reported in a previous study.[5] Jarosite is known to be a sink for metals (Pb, Zn, Cu)[47] formed in AMD environments due to the oxidation of sulfidic minerals.[33, 48, 49] Enhancing oxidation of Fe(II) minerals in AMD has been shown to be effective in removing heavy metals from solution by sequestration in jarosite.[50, 51] The stability of jarosite can be affected by pH,[52, 53] metal substitution[54] and association with other minerals.[55] Furthermore, the geochemical weathering increases the bioavailability of the metal-bearing minerals; thus, metal-bearing jarosite poses a higher risk for exposure than unweathered minerals.[14–16, 53] Overall, jarosite is not thermodynamically stable at circumneutral pH; hence, jarosite will likely dissolve at pH values higher than 6 detected downstream of CC in the AR,[52, 53] releasing the associated metals to the environment. Spikes in Pb concentrations due to an increase in pH and oxidation of Fe(II) oxides have been predicted by a reactive transport model and measured in the MC upstream the AR,[56, 57] which support the association of Pb with a pH-dependent Fe mineral. However, there are several pathways that the released metals can follow once in the environment, among them: a) sorption into other mineral phases (*e.g.* Pb and Zn sorption onto hydrous ferric oxide) [58–60]; b) interaction and immobilization with soil organic matter (*e.g.* Cr complexation with natural organic matter[61]); or, c) complexation with dissolved organic matter and remain in the aqueous phase[62, 63].

Environmental implications

Spectroscopy and microscopy analyses show the association of Pb, Cu, and Zn with Fe-minerals such as jarosite, goethite, and clays in sediments from CC and BB. Metal concentrations in water (e.g., As and Pb) exceed national drinking water standards during high flow events along the AR (Figure S1). The increase in the duration and intensity of heavy precipitation events with the changing climate in the Southwestern US57 could contribute to the resuspension of deposited sediments and mobilization of heavy metals. More information is necessary to assess the effect of snowmelt and rain on metal remobilization from sediments in river basins in semi-arid regions. The unique metal mixtures identified in sediments analyzed in this study show that they come from diverse sources (natural mineralization and mining activities). The weathering of minerals in sediments can increase metal bioavailability in the AR ecosystem; studies have reported that jarosite is more bioavailable than goethite through ingestion and inhalation.[14–16, 53] Finally, the high nutrient loads in water and sediments from intense farming in Farmington, NM, could contribute to oxygen depletion, affecting the redox cycle sensitive metals (e.g., Fe, Mn, As, U). Metal accumulation in crops and plants after irrigation is a relevant exposure pathway in active agricultural areas. Hence, future research should focus on better understanding the interaction of metal-bearing minerals and nutrients in water and sediments to further assess biogeochemical release and accumulation of metals in the AR.

Author Manuscript Author Manuscript Author Manuscript Author Manuscript

Supplementary Material

Refer to Web version on PubMed Central for supplementary material.

Acknowledgments

The authors would like to thank Dennis McQuillan for his feedback and support, and Katie Zemlick for developing the maps. Special thanks to Jesus Gomez-Velez, Daniel Cadol, and Andrew Luhmann from New Mexico Tech for organizing the sampling trip to Animas River. Finally, we thank the National Institute of Health Centers of Excellence on Environmental Health Disparities Research (Grant number 1-P50-ES-026102-01), the National Science Foundation under New Mexico EPSCoR (Grant number IIA-1301346), and CREST (Grant number 1345169) for providing the funding for this research. Any opinions, findings, conclusions or recommendations expressed in this publication are those of the author(s) and do not necessarily reflect the views of the National Science Foundation.

References

1. Benner SG, Blowes DW, Gould WD, Herbert RB, Ptacek CJ. Geochemistry of a Permeable Reactive Barrier for Metals and Acid Mine Drainage. Environ. Sci. Technol. 1999; 33(16):2793–2799.
2. U.S. Department of the Interior, Bureau of Land Management. Abandoned mine lands – A New legacy. May. 2013 Report number: BLM/WO/GI-13/007-3720
3. Buxton, HT., Nimick, DA., Guerard, Pv, Church, SE., Frazier, AG., Gray, JR., Lipin, BR., Marsh, SP., Woodward, DF., Kimball, BA., Finger, SE., Ischinger, LS., Fordham, JC., Power, MS., Bunck, CM., Jones, JW. A science-based, watershed strategy to support effective remediation of abandoned mine lands; Fourth International Conference on Acid Rock Drainage (ICARD); Vancouver, British Columbia, Canada. 1997. p. 1869-1880.
4. Bove, DJ., Hon, K., Budding, KE., Slack, JF., Snee, LW., Yeoman, RA. Geochronology and geology of late Oligocene through Miocene volcanism and mineralization in the Western San Juan Mountains. Colorado: U.S. Geological Survey Professional Paper 1642; 2001.
5. Bove, DJ., Mast, MA., Dalton, JB., Wright, WG., Yager, DB. Major styles of mineralization and hydrothermal alteration and related solid- and aqueous-phase geochemical signatures. In: Church, SE.Von Guerard, P., Finger, SE., editors. Integrated investigations of environmental effects of historical mining in the Animas River Watershed. San Juan County, Colorado: U.S. Geological Survey Professional Paper 1651; 2007. p. 165-230.
6. Church, SE., Fey, DL., Blair, R. Icard, Pre-mining bed sediment geochemical baseline in the Animas River watershed, Southwestern Colorado. Soc Mining Metallurgy and Exploration Inc; Littleton: 2000. p. 499-512.
7. Church, SE., Owen, JR., von Guerard, P., Verplanck, PL., Kimball, BA., Yager, DB. The effects of acidic mine drainage from historical mines in the Animas River watershed, San Juan County, Colorado-What is being done and what can be done to improve water quality?. In: DeGraff, JV., editor. understanding and responding to hazardous substances at mine sites in the Western United States. Vol. 17. Geological Soc Amer Inc; Boulder: 2007. p. 47-83.
8. Church, SE.Von Guerard, P., Finger, SE., editors. Integrated investigations of environmental effects of historical mining in the Animas River watershed. San Juan County, Colorado: U.S. Dept. of the Interior, U.S. Geological Survey: Reston, Va; 2007.
9. Mast, MA., Verplanck, PL., Yager, DB., Wright, WG., Bove, DJ. Icard, Natural sources of metals to surface waters in the upper Animas River watershed, Colorado. Soc Mining Metallurgy and Exploration Inc; Littleton: 2000. p. 513-522.
10. U.S. Department of the Interior, Bureau of Reclamation. Technical evaluation of the Gold King Mine incident. Reclamation, managing water in the West; 2015.
11. Chen, Y-t, Li, J-t, Chen, L-x, Hua, Z-s, Huang, L-n, Liu, J., Xu, B-b, Liao, B., Shu, W-s. Biogeochemical processes governing natural pyrite oxidation and release of acid metalliferous drainage. Environ. Sci. Technol. 2014; 48(10):5537–5545. [PubMed: 24730689]

Author Manuscript Author Manuscript Author Manuscript Author Manuscript

12. Baken S, Salaets P, Desmet N, Seuntjens P, Vanlierde E, Smolders E. Oxidation of iron causes removal of phosphorus and arsenic from streamwater in groundwater-fed lowland catchments. Environ. Sci. Technol. 2015; 49(5):2886–2894. [PubMed: 25661567]
13. Dai C, Hu Y. Fe(III) hydroxide nucleation and growth on quartz in the presence of Cu(II), Pb(II), and Cr(III): metal hydrolysis and adsorption. Environ. Sci. Technol. 2015; 49(1):292–300. [PubMed: 25496643]
14. Kimball BE, Foster AL, Seal RR, Piatak NM, Webb SM, Hammarstrom JM. Copper speciation in variably toxic sediments at the Ely Copper Mine, Vermont, United States. Environ. Sci. Technol. 2016; 50(3):1126–1136. [PubMed: 26734712]
15. Hayes SM, Webb SM, Bargar JR, O'Day PA, Maier RM, Chorover J. Geochemical weathering increases lead bioaccessibility in semi-arid mine tailings. Environ. Sci. Technol. 2012; 46(11): 5834–5841. [PubMed: 22553941]
16. Schaider LA, Senn DB, Brabander DJ, McCarthy KD, Shine JP. Characterization of zinc, lead, and cadmium in mine waste: Implications for transport, exposure, and bioavailability. Environ. Sci. Technol. 2007; 41(11):4164–4171. [PubMed: 17612206]
17. Kimball BA, Runkel RL, Walton-Day K. An approach to quantify sources, seasonal change, and biogeochemical processes affecting metal loading in streams: Facilitating decisions for remediation of mine drainage. Appl. Geochem. 2010; 25(5):728–740.
18. Cerkez EB, Bhandari N, Reeder RJ, Strongin DR. Coupled redox transformation of chromate and arsenite on ferrihydrite. Environ. Sci. Technol. 2015; 49(5):2858–2866. [PubMed: 25658969]
19. Pierre Louis A-M, Yu H, Shumlas SL, Van Aken B, Schoonen MAA, Strongin DR. Effect of phospholipid on pyrite oxidation and microbial communities under simulated acid mine drainage (AMD) conditions. Environ. Sci. Technol. 2015; 49(13):7701–7708. [PubMed: 26018867]
20. U.S. Environmental Protection Agency. https://www.epa.gov/goldkingmine/data-gold-king-mine-response#samplingdataresults
21. U.S. Geological Survey. NWISWeb Data for the Nation (US Geol Surv, Reston, VA). http://waterdata.usgs.gov/nwis
22. Wright, WG., Simon, W., Bove, DJ., Mast, MA., Leib, KJ. Distribution of pH values and dissolved trace-metal concentrations in streams. In: Church, SE.Von Guerard, P., Finger, SE., editors. Integrated investigations of environmental effects of historical mining in the Animas River Watershed. San Juan County, Colorado: U.S. Geological Survey Professional Paper 1651; 2007. p. 501-541.
23. Mast, MA., Verplanck, PL., Wright, WG., Bove, DJ. Characterization of background water quality. In: Church, SE.Von Guerard, P., Finger, SE., editors. Integrated investigations of environmental effects of historical mining in the Animas River Watershed. San Juan County, Colorado: U.S. Geological Survey Professional Paper 1651; 2007. p. 351-386.
24. U.S. Geological Survey. Water Quality Samples for the Nation. USGS 09364500 Animas River At Farmington, NM: Dec. 2015 As of
25. U.S. Geological Survey. Water Quality Samples for the Nation. USGS 09365000 San Juan River at Farmington, NM: Dec. 2015 As of
26. Kimball, BA., Walton-Day, K., Runkel, RL. Quantification of metal loading by tracer injection and synoptic sampling, 1996–2000. In: Church, SE.Von Guerard, P., Finger, SE., editors. Integrated investigations of environmental effects of historical mining in the Animas River watershed. San Juan County, Colorado: U.S. Geological Survey Professional Paper 1651; 2007. p. 423-495.
27. Taylor SR. Abundance of chemical elements in the continental crust - A new table. Geochim. Cosmochim. Acta. 1964 Aug.28:1273–1285.
28. Church, SE., Fey, DL., Unruh, DM. Trace elements and lead isotopes in modern streambed and terrace sediment - Determination of current and premining geochemical baselines. In: Church, SE.Von Guerard, P., Finger, SE., editors. Integrated investigations of environmental effects of historical mining in the Animas River Watershed. San Juan County, Colorado: U.S. Geological Survey Professional Paper 1651; 2007. p. 575-642.
29. Theis, NJ., Madson, ME., Rosenlund, GC., Reinhart, WR., Gardner, HA. National uranium resource evaluation: Durango Quadrangle, Colorado (GJQ--011-81). International Nuclear Information System; United States: 1981. p. 145

Author Manuscript Author Manuscript Author Manuscript Author Manuscript

30. U.S. Department of Energy; Durango, Colorado, Processing and Disposal Sites. Legacy Management. 2015. http://www.lm.doe.gov/Durango/Processing/Documents.aspx
31. Casadevall T, Ohmoto H. Sunnyside Mine, Eureka mining district, San Juan County, Colorado, geochemistry of gold and base metal ore deposition in a volcanic environment. Econ. Geol. 1977; 72(7):1285–1320.
32. Frost RL, Wills R-A, Weier ML, Martens W, Mills S. A Raman spectroscopic study of selected natural jarosites. Spectrochim. Acta A. 2006; 63(1):1–8.
33. Hochella MF, Moore JN, Golla U, Putnis A. A TEM study of samples from acid mine drainage systems: Metal-mineral association with implications for transport. Geochim. Cosmochim. Acta. 1999; 63(19–20):3395–3406.
34. van der Zee C, Roberts DR, Rancourt DG, Slomp CP. Nanogoethite is the dominant reactive oxyhydroxide phase in lake and marine sediments. Geology. 2003; 31:993–996.
35. Yoshida, Y., Langouche, G. Mössbauer spectroscopy: Tutorial book. Vol. 2013. Springer-Verlag Berlin Heidelberg; 2013. Mössbauer spectroscopy; p. 1
36. Murad, E., Cashion, J. Mössbauer spectroscopy of environmental materials and their industrial utilization. Kluwer Academic Publishers; 2004.
37. Dyar MD, Agresti DG, Schaefer MW, Grant CA, Sklute EC. Mossbauer spectroscopy of earth and planetary elements. Annu. Rev. Earth Planet. Sci. 2006; 34:83–125.
38. Dyar MD, Schaefer MW, Sklute EC, Bishop JL. Mossbauer spectroscopy of phyllosilicates: effects of fitting models on recoil-free fractions and redox ratios. Clay Miner. 2008; 43(1):3–33.
39. Dutrizac J, Kaiman S. Synthesis and properties of jarosite-type compounds. Can. Mineral. 1976; 14(2):151–158.
40. Church SE, Fey DL, Unruh DM, Vaughn RB, Taggart JE Jr. Geochemical and isotopic data from streambed sediment, Animas River watershed, Colorado, 1995–1999. 2000:2000–244.
41. Nania, J., Cozzetto, K., Duren, S. Chapter 5 - Farming. In: Nania, J., Cozzetto, K., editors. Considerations for climate change and variability adaptation on the Navajo Nation. University of Colorado, Boulder, CO; 2014.
42. Carpenter SR, Caraco NF, Correll DL, Howarth RW, Sharpley AN, Smith VH. Nonpoint pollution of surface waters with phosphorus and nitrogen. Ecol. Appl. 1998; 8(3):559–568.
43. Servin AD, Morales MI, Castillo-Michel H, Hernandez-Viezcas JA, Munoz B, Zhao L, Nunez JE, Peralta-Videa JR, Gardea-Torresdey JL. Synchrotron verification of TiO_2 accumulation in cucumber fruit: a possible pathway of TiO_2 nanoparticle transfer from soil into the food chain. Environ. Sci. Technol. 2013; 47(20):11592–11598. [PubMed: 24040965]
44. Zhao L, Sun Y, Hernandez-Viezcas JA, Hong J, Majumdar S, Niu G, Duarte-Gardea M, Peralta-Videa JR, Gardea-Torresdey JL. Monitoring the environmental effects of CeO_2 and ZnO nanoparticles through the life cycle of corn (Zea mays) plants and in situ μ-XRF mapping of nutrients in kernels. Environ. Sci. Technol. 2015; 49(5):2921–2928. [PubMed: 25648544]
45. Zhou H, Yang WT, Zhou X, Liu L, Gu JF, Wang WL, Zou JL, Tian T, Peng PQ, Liao BH. Accumulation of heavy metals in vegetable species planted in contaminated soils and the health risk assessment. Int. J. Environ. Res. Public Health. 2016; 13(3)
46. Dalton, JB., Bove, DJ., Mladinich, CS., Rockwell, BW. Imaging spectroscopy applied to the Animas River Watershed and Silverton Caldera. In: Church, SE.Von Guerard, P., Finger, SE., editors. Integrated investigations of environmental effects of historical mining in the Animas River watershed. San Juan County, Colorado: U.S. Geological Survey Professional Paper 1651; 2007. p. 141-159.
47. Dutrizac JE, Dinardo O. The co-precipitation of copper and zinc with lead jarosite. Hydrometallurgy. 1983; 11(1):61–78.
48. Hochella MF, Moore JN, Putnis CV, Putnis A, Kasama T, Eberl DD. Direct observation of heavy metal-mineral association from the Clark Fork River Superfund Complex: Implications for metal transport and bioavailability. Geochim. Cosmochim. Acta. 2005; 69(7):1651–1663.
49. Elwood Madden ME, Bodnar RJ, Rimstidt JD. Jarosite as an indicator of water-limited chemical weathering on Mars. Nature. 2004; 431(7010):821–823. [PubMed: 15483605]
50. Tucci NJ, Gammons CH. Influence of copper recovery on the water quality of the acidic Berkeley Pit Lake, Montana, USA. Environ. Sci. Technol. 2015; 49(7):4081–4088. [PubMed: 25723275]

Author Manuscript Author Manuscript Author Manuscript Author Manuscript

51. Webster JG, Swedlund PJ, Webster KS. Trace metal adsorption onto an acid mine drainage iron(III) oxy hydroxy sulfate. Environ. Sci. Technol. 1998; 32(10):1361–1368.
52. Arslan C, Arslan F. Thermochemical review of jarosite and goethite stability regions at 25°C and 95°C. Turkish J. Eng. Env. Sci. 2003; 27:45–52.
53. Hayes SM, White SA, Thompson TL, Maier RM, Chorover J. Changes in lead and zinc lability during weathering-induced acidification of desert mine tailings: Coupling chemical and micro-scale analyses. App. Geochem. 2009; 42(12):2234–2245.
54. Kendall MR, Madden AS, Madden MEE, Hu QH. Effects of arsenic incorporation on jarosite dissolution rates and reaction products. Geochim. Cosmochim. Acta. 2013; 112:192–207.
55. Brown JB. Jarosite-geoethite stabilities at 25 °C, 1 ATM. Miner. Deposita. 1971; 6(3):245–252.
56. Runkel RL, Kimball BA. Evaluating remedial alternatives for an acid mine drainage stream: Application of a reactive transport model. Environ. Sci. Technol. 2002; 36(5):1093–1101. [PubMed: 11917996]
57. Runkel RL, Kimball BA, Waton-Day K, Verplanck PL, Broshears RE. Evaluating remedial alternatives for an acid mine drainage stream: a model post audit. Environ. Sci. Technol. 2012; 46(1):340–347. [PubMed: 22074087]
58. Runkel RL, Kimball BA, McKnight DM, Bencala KE. Reactive solute transport in streams: A surface complexation approach for trace metal sorption. Water Resour. Res. 1999; 35(12):3829–3840.
59. Schemel LE, Kimball BA, Runkel RL, Cox MH. Formation of mixed Al-Fe colloidal sorbent and dissolved-colloidal partitioning of Cu and Zn in the Cement Creek - Animas River Confluence, Silverton, Colorado. Appl. Geochem. 2007; 22(7):1467–1484.
60. Karapınar N. Removal of heavy metal ions by ferrihydrite: an opportunity to the treatment of acid mine drainage. Wate Air Soil Pollut. 2016; 227(6):1–8.
61. Gustafsson JP, Persson I, Oromieh AG, van Schaik JWJ, Sjöstedt C, Kleja DB. Chromium(III) complexation to natural organic matter: mechanisms and modeling. Environ. Sci. Technol. 2014; 48(3):1753–1761. [PubMed: 24422446]
62. Craven AM, Aiken GR, Ryan JN. Copper(II) binding by dissolved organic matter: importance of the copper-to-dissolved organic matter ratio and implications for the biotic ligand model. Environ. Sci. Technol. 2012; 46(18):9948–9955. [PubMed: 22871072]
63. Sharma P, Rolle M, Kocar B, Fendorf S, Kappler A. influence of natural organic matter on As transport and retention. Environ. Sci. Technol. 2011; 45(2):546–553. [PubMed: 21142173]

Author Manuscript Author Manuscript Author Manuscript Author Manuscript

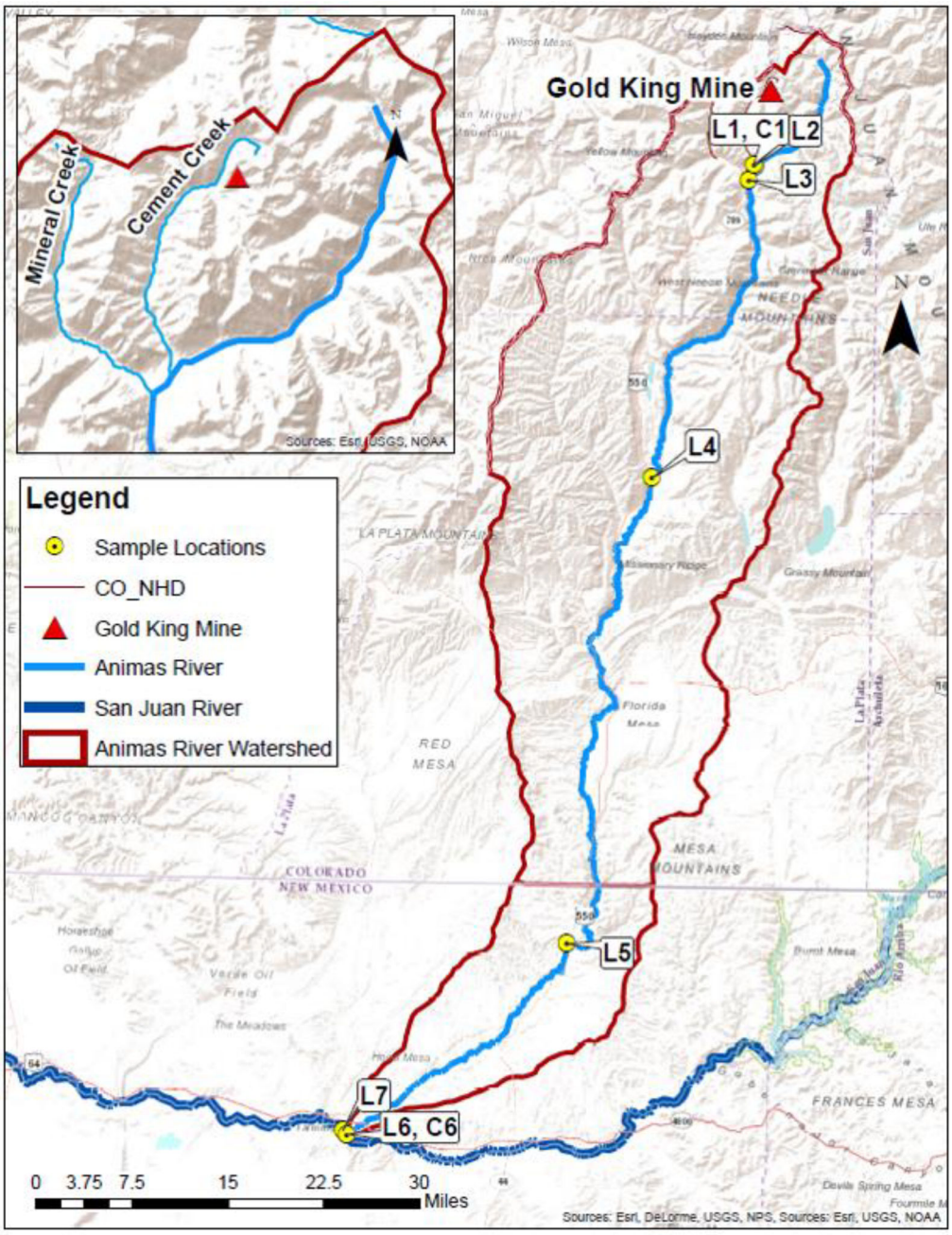

Figure 1.

Map of the Animas River watershed from upstream Silverton to its confluence with the San Juan River. The map includes the Gold King Mine location by the Cement Creek and the sampling locations. The small box is the magnification of the area around the red triangle to highlight two tributaries of the Animas River, Cement Creek and Mineral Creek.

Author Manuscript Author Manuscript Author Manuscript Author Manuscript

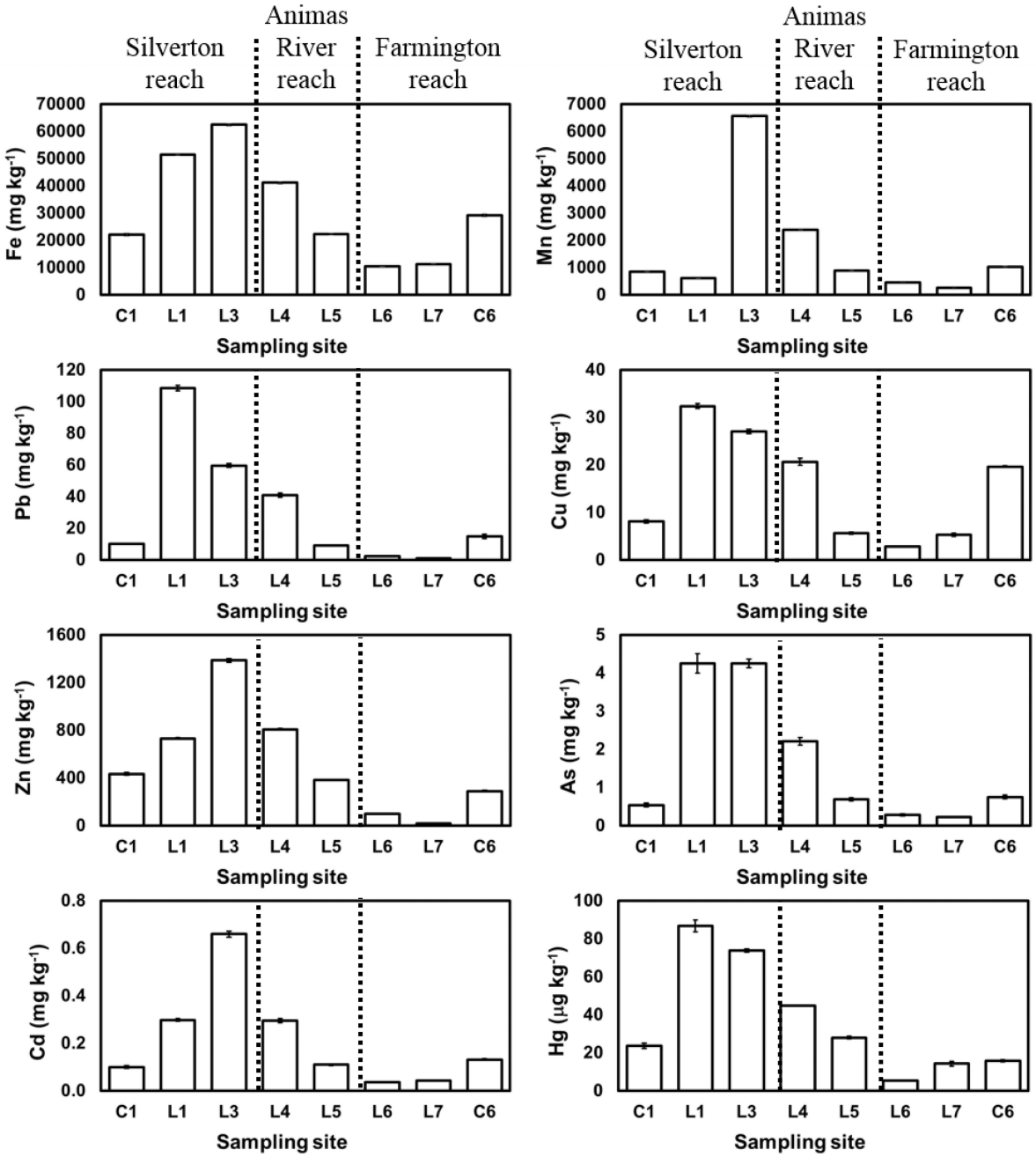

Figure 2.

Selected metal concentrations in the sediment samples after digestion in triplicate of the sediments with aqua regia. The error bars are plotted in all figures and they are the standard deviation of the triplicates.

Author Manuscript Author Manuscript Author Manuscript Author Manuscript

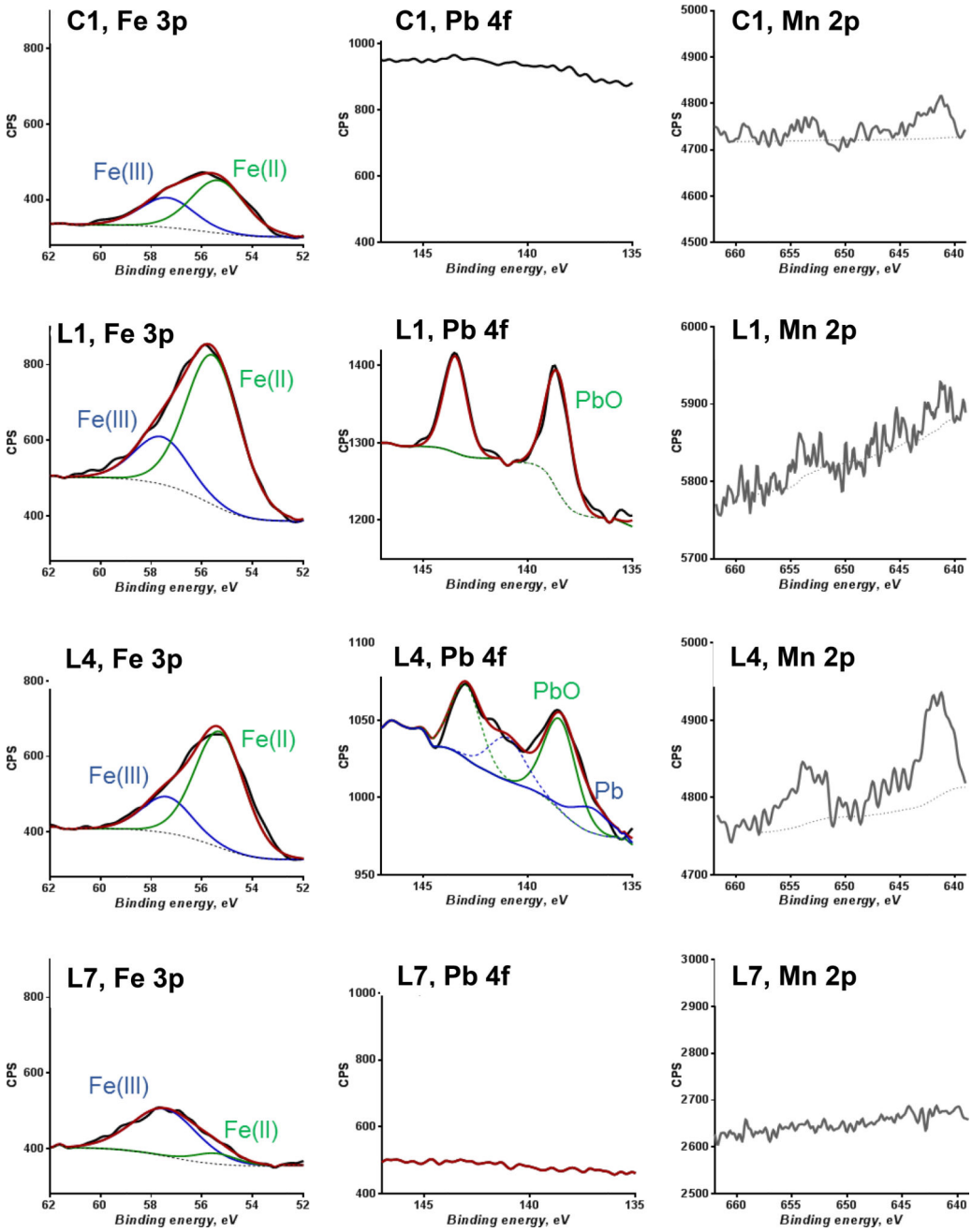

Figure 3.

X-ray photoelectron spectra (XPS) of iron (Fe), lead (Pb), and manganese (Mn) for the sediment samples C1, L1, L4, and L7.

Author Manuscript Author Manuscript Author Manuscript Author Manuscript

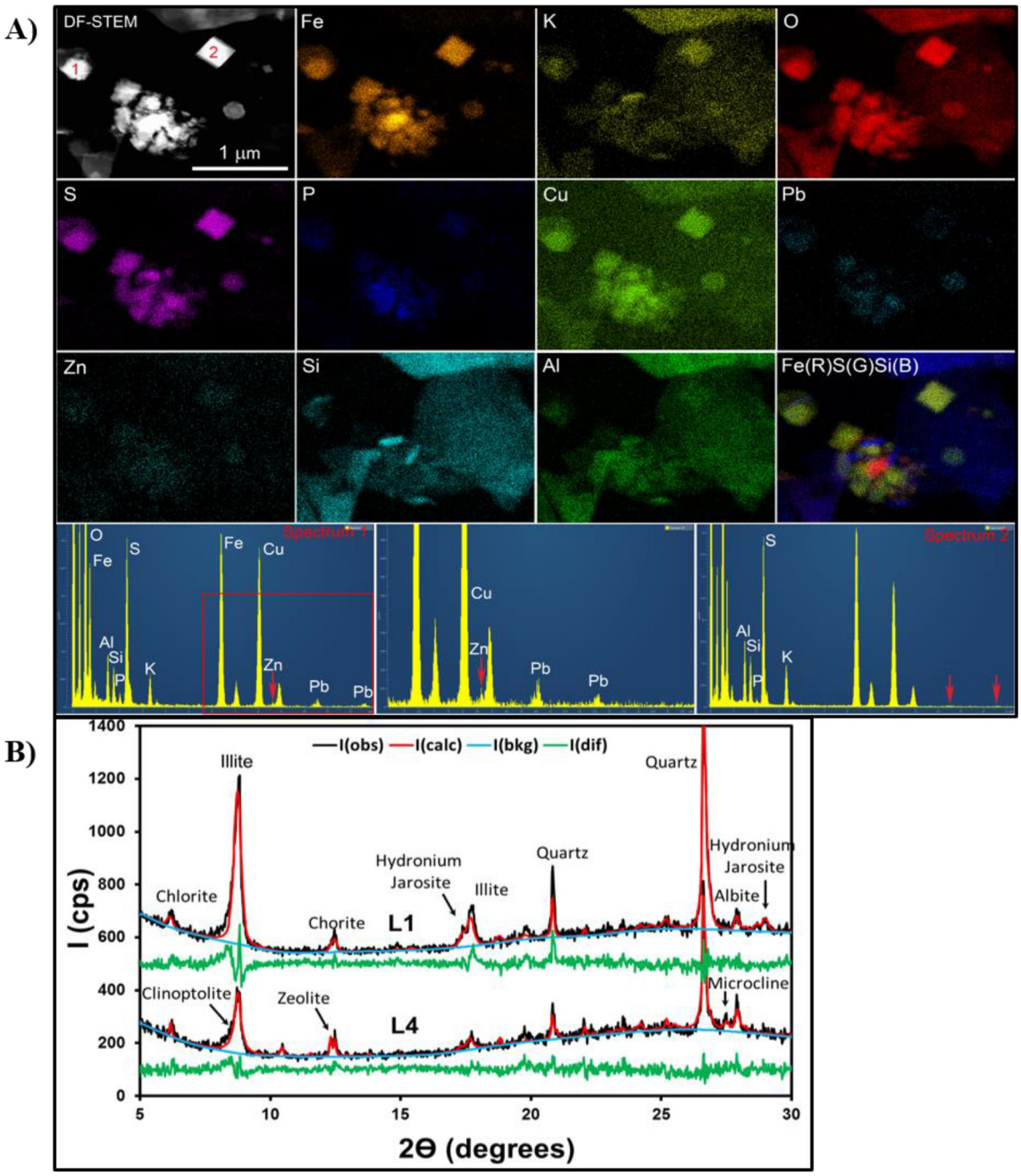

Figure 4.

Mineralogy of the sediments. Panel **A** shows the scanning transmission electron microscope (STEM) and STEM X-ray map data of crystals in sediment sample from Cement Creek, L1. Upper left image is a dark-field STEM image showing two submicron, euhedral crystals of jarosite (bright in the image and labeled as **1** and **2**), associated with fine-grained, clay-rich material and Fe-oxyhydroxides (center part of the image). Additional images show STEM X-ray maps for Fe, K, O, S, P, Cu, Pb, Zn, Si and Al. The intensity of the color is correlated with the concentration of the element in the sample. The data show that in addition to the major elements, Fe, K, Cu, O, and S, the jarosite grain **1** also contain detectable

concentrations of P, Pb and Zn, but they are not detected in jarosite grain **2**. This data is supported by the EDS spectra presented in the bottom of the image. Panel **B** is the X-ray diffraction spectra of samples from Cement Creek, L1, and Baker's Bridge, L4.

Author Manuscript Author Manuscript Author Manuscript Author Manuscript

Author Manuscript Author Manuscript Author Manuscript Author Manuscript

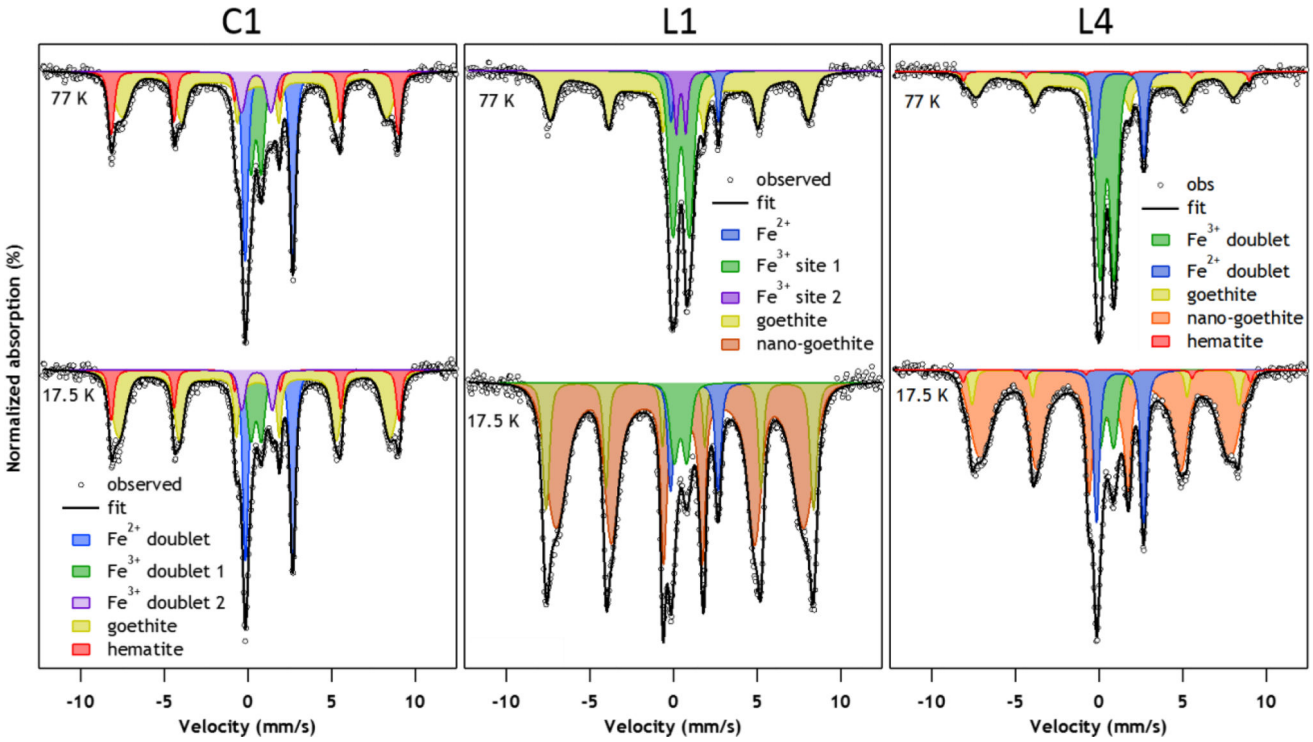

Figure 5.

Mössbauer spectra of Animas River sediment samples at 77 K and 17.5 K. The samples analyzed are from Cement Creek, C1 (panel **A**) and L1 (panel **B**); and, from BB, L4 (panel **C**), and sample C1 at 77 K and 17.5 K.